
International Journal of Mechanics and Materials in Design **1:** 157–171, 2004.

Compliant mechanism design with non-linear materials using topology optimization

DAEYOON JUNG and HAE CHANG GEA*

Department of Mechanical and Aerospace Engineering, Rutgers, The State University of New Jersey, Piscataway, NJ 08854, USA
**Author for correspondence (E-mail: gea@rci.rutgers.edu)*

Received 25 March 2003; accepted in revised form 24 June 2004

Abstract. In this paper, compliant mechanism design with non-linear materials using topology optimization is presented. A general displacement functional with non-linear material model is used in the topology optimization formulation. Sensitivity analysis of this displacement functional is derived from the adjoint method. Optimal compliant mechanism examples for maximizing the mechanical advantage are presented and the effect of non-linear material on the optimal design are considered.

Key words: compliant mechanism, sensitivity analysis, topology optimization

1. Introduction

Traditional mechanism design is accomplished by using many rigid components and kinematics joints. As the manufacturing and assembly cost increases with the number of components used, a special class of single component mechanism called *compliant mechanism* that can perform the similar functionalities by utilizing the elastic deformation has drawn much attention in recent years (Howell and Midha, 1993; Ananthasuresh et al., 1994; Ananthasuresh and Kota, 1996; Sigmund, 1997; Larsen et al., 1997; Pedersen Yin and Ananthasuresh, 2002). Design of compliant mechanism using topology optimization was first introduced by Ananthasuresh et al. (1994). Later, research on compliant mechanism with topology optimization was extended to various optimization formulations considering the structural compliance (the maximization of the mutual strain energy) and the structural rigidity (the minimization of the strain energy). A multi-criteria formulation of maximizing the mutual strain energy and minimizing the strain energy was studied by Frecker et al. (1997). A weighted sum formulation of these energy terms was proposed by Nishiwaki et al. (1998). A power ratio formulation of the mutual strain energy and the strain energy was used by Saxena and Ananthasuresh (2000).

Although many successful examples of compliant mechanism design by the topology optimization formulation were reported, most of the designs were based on the linear material model with geometrical non-linearity only. The use of linear material model may not be valid in practice because materials with large compliance often exhibit non-linear behavior (Jog, 1996; Buhl et al., 2000; Bruns and Tortorelli, 2001; Bruns et al., 2002; Pedersen et al., 2001; Sigmund, 2001a, b). Material non-linearity is due to the non-linear elastic or plastic behavior of the structural material. Despite the maturity of non-linear material analysis, the main challenge of implementing non-linear material model in the topology optimization is in the computational efficiency of the sensitivity analysis. Comparing with vast publications on

topology optimization with linear materials, very limited research works can be found on non-linear materials. Song (1986) used a simplified non-linear spring to model non-linear elastic–plastic problems. Design sensitivity of the global plate thickness of an elastic–plastic structural optimization was studied by Vander Lugt et al. (1987). Bendsøe et al. (1996) developed a non-linear softening material for structural topology optimization. Pedersen (1998) developed a power law non-linear material model for rigidity based topology optimization. An elastic-perfectly-plastic material model was studied by Swan and Kosaka (1997), and Swan and Arora (1997); an elastoplastic material model with linear work-hardening were considered by Yuge and Kikuchi (1995), and by Maute et al. (1998). However, a more general non-linear material model for compliant mechanism design using topology optimization has not yet, to our knowledge, been reported.

In this paper, compliant mechanism design with non-linear materials using topology optimization is presented. A general displacement functional with non-linear material model is used in the topology optimization formulation. Sensitivity analysis of this displacement functional is derived from the adjoint method and the optimization problem is solved iteratively by the generalized convex approximation (GCA) (Chickermane and Gea 1996). In order to consider material non-linearity, a power law non-linear material model and an elastomer like material model are used. However, the derivations presented here can be extended to other non-linear material models without much alteration. In Section 2, a brief discussion on non-linear material models will be given. Then, sensitivity analysis of a general displacement functional will be derived. Optimal compliant mechanism examples, for maximizing the mechanical advantage which is a special form of displacement functional are presented before the concluding remarks.

2. Analysis with material non-linearity

Most engineering materials exhibit non-linear behavior when the deformation is sufficiently large. The design of a compliant mechanism should take into account the material non-linearity into account because the functionalities of the compliant mechanism are accomplished from its large deformation. Many material models have been proposed to describe the material non-linearity; a complete references can be found in the monograph by Chen (1994). In this section, we will briefly discuss the role of non-linear material model in finite element analysis. Non-linear material model will be reviewed in the first part and then linearized incremental analysis will be discussed. For more complete discussion on this subject, please refer to the book by Belytschko et al. (2000).

2.1. Constitutive equation for non-linear material model

In order to construct the constitutive equation, the stress and strain tensors are transformed into the effective stress and strain as follows:

$$\sigma_{\mathrm{e}}^2 = \sigma_{ij}\, C_{ijkl}^{0\ -1}\, \sigma_{kl}, \tag{1}$$

$$\varepsilon_{\mathrm{e}}^2 = \varepsilon_{ij}\, C_{ijkl}^{0}\, \varepsilon_{kl}, \tag{2}$$

where σ_e and ε_e denote the effective stress and strain; σ_{ij} and ε_{ij} represent the stress and strain tensors and C^0_{ijkl} is a positive definite and dimensionless matrix. The relation between the effective stress and the effective strain is defined as follows:

$$\sigma_e = Kf(\varepsilon_e), \tag{3}$$

where function $f(\varepsilon_e)$ is a function representing the material characteristics and K is a constant reference modulus of material. This material model is very flexible. Based on the selection of $f(\varepsilon_e)$ linear materials, power-law materials or even elastomer like materials can be modeled. Because the strain energy density must be consistent regardless of the strain and stress used, we have the following relation:

$$u = \int_0^{\varepsilon_{ij}} \sigma_{ij}\,\mathrm{d}\varepsilon_{ij} = \int_0^{\varepsilon_e} \sigma_e\,\mathrm{d}\varepsilon_e, \tag{4}$$

where u denotes the strain energy density. By taking the derivative of Eq. (2), we have $\varepsilon_e\,\mathrm{d}\varepsilon_e = \varepsilon_{ij}C^0_{ijkl}\,\mathrm{d}\varepsilon_{kl}$. Substituting the result into Eq. (4) and replacing σ_e with $Kf(\varepsilon_e)$ from Eq. (3), we have the constitutive equation in the form of

$$\begin{aligned}\sigma_{ij} &= K(f(\varepsilon_e)/\varepsilon_e)\,C^0_{ijkl}\,\varepsilon_{kl}\\ &= Kg(\varepsilon_e)\,C^0_{ijkl}\,\varepsilon_{kl},\end{aligned} \tag{5}$$

where $g(\varepsilon_e) = f(\varepsilon_e)/\varepsilon_e$. Since the stress at ε_p from Eq. (5) is equal with that from linear elastic constitutive relation at ε_p, reference modulus of material (K) can be obtained as $K = E/g(\varepsilon_p)$ in which E is a Young's modulus and ε_p is the strain at which non-linear behavior is initiated.

2.2. Linearized incremental analysis

When the response of a structure subjected to body forces, f_i^B, surface tractions, f_i^s on the surface S_{fi} and displacement boundary conditions, S_u is considered, its behavior is obtained by solving equilibrium equation, the strain-displacement relation, and the constitutive equation. Equation (5) will be used as the constitutive equation for the non-linear material model. And a principle of virtual displacements will be used as an equilibrium equation in a weak form.

$$\int_v \sigma_{ij}\,\delta\varepsilon_{ij}\,\mathrm{d}V = \int_v f_i^B \delta u_i\,\mathrm{d}V + \int_S f_i^S \delta u_i^S\,\mathrm{d}S. \tag{6}$$

The strain–displacement relation is assumed to be linear such that:

$$\varepsilon_{ij} = \frac{1}{2}\left(\frac{\partial u_i}{\partial x_j} + \frac{\partial u_j}{\partial x_i}\right). \tag{7}$$

The equilibrium equation cannot be solved directly due to the non-linearity in constitutive equation. It is solved iteratively by using incrementally linearized equations. In the incremental analysis, the responses of structure are calculated by adding linear responses occurred during the incremental configuration change to that of the current state (Bathe, 1996). The responses at current configuration state can be obtained by incrementally accumulating the responses from the initial state to the current state. When the change in displacement under

incremental forces is Δu_i, increments in strain are obtained by replacing u_i with $u_i + \Delta u_i$ in Eq. (7).

$$\Delta\varepsilon_{ij} = \frac{1}{2}\left(\frac{\partial \Delta u_i}{\partial x_j} + \frac{\partial \Delta u_j}{\partial x_i}\right). \tag{8}$$

The stress, σ_{ij}, at the incremented state is obtained by adding the incremental stress $(\Delta\sigma_{ij})$ occurred during strain increment $(\Delta\varepsilon_{kl})$ to the stress (σ_{ij}) at current state.

$$\begin{aligned}\sigma_{ij}^{t+\Delta t} &= \sigma_{ij}^{t} + \Delta\sigma_{ij} \\ &= \sigma_{ij}^{t} + \frac{\partial \sigma_{ij}}{\partial \varepsilon_{kl}}\Delta\varepsilon_{kl} \\ &= \sigma_{ij}^{t} + C_{ijkl}^{\tan}\Delta\varepsilon_{kl},\end{aligned} \tag{9}$$

where the $C_{ijkl}^{\tan}$ is the tangent modulus tensor at the current strain (ε_{kl}) and it can be obtained by taking the derivative of the constitutive equation of the non-linear material, Eq. (5), about strain, ε_{kl}, as follows:

$$\begin{aligned}C_{ijkl}^{\tan} &= Kg(\varepsilon_{\mathrm{e}})C_{ijkl}^{0} + K\frac{1}{\varepsilon_{\mathrm{e}}}\frac{\partial g(\varepsilon_{\mathrm{e}})}{\partial \varepsilon_{\mathrm{e}}}C_{ijkl}^{0}\varepsilon_{kl}\frac{\partial \varepsilon_{\mathrm{e}}}{\partial \varepsilon_{kl}} \\ &= Kg(\varepsilon_{\mathrm{e}})C_{ijkl}^{0} + K\frac{1}{\varepsilon_{\mathrm{e}}}\frac{\partial g(\varepsilon_{\mathrm{e}})}{\partial \varepsilon_{\mathrm{e}}}C_{ijpq}^{0}\varepsilon_{pq}\varepsilon_{rs}C_{rskl}^{0}.\end{aligned} \tag{10}$$

After obtaining the tangent modulus tensor at any given state, the incremental stress state can then be calculated from Eq. (9) as $\Delta\sigma_{ij} = C_{ijkl}^{\tan}\Delta\varepsilon_{kl}$.

Now the linearized equilibrium equation is obtained by replacing σ_{ij} with Eq. (9) and $\delta\varepsilon_{ij}$ with $\delta\Delta\varepsilon_{ij}$ because strain at current state is a reference state for the incremental analysis.

$$\int_V C_{ijkl}^{\tan}\Delta\varepsilon_{ij}\,\delta\Delta\varepsilon_{kl}\,\mathrm{d}V = R - \int_V \sigma_{ij}\delta\varepsilon_{ij}\,\mathrm{d}V, \tag{11}$$

where R is the virtual work of all external forces. The right hand-side of the above equation represents "out-of-balance virtual work" after analysis for the current structure. This "out of balance" arises from the linearization and the analysis should be repeated until the difference is less than the satisfactory level. When the above equation is written in the discretized form of FEM, the first term can be described as same as that of linear analysis with replacing constitutive matrix with tangent modulus matrix.

3. Design sensitivity analysis

One of the most commonly used functionals in structural optimization is the displacement functional. Some examples of displacement functional are the mean compliance for stiffness design, the regional strain energy for energy absorption design, and the geometric advantage (GA)/the mechanical advantage (MA) for compliant mechanism design. In this section, sensitivity analysis of a general displacement functional will be derived using the adjoint method.

Consider a general displacement functional, H, as

$$H = \int_V h(u_i, p)\,\mathrm{d}V, \tag{12}$$

where u_i denotes the displacement field and p represents the design variable. To derive the sensitivity of the displacement functional, we introduce a new functional, H^* by adding the strain-displacement relation, the constitutive equation of the non-linear material model, and the equilibrium equation of the structure to the displacement functional, H, as

$$\begin{aligned} H^* = H &+ \int_V \sigma_{ij}^{\mathrm{a}}\left(\varepsilon_{ij} - \frac{1}{2}\left(\frac{\partial u_i}{\partial x_j} + \frac{\partial u_j}{\partial x_i}\right)\right)\mathrm{d}V \\ &+ \int_V \varepsilon_{ij}^{\mathrm{a}}(\sigma_{ij} - K g(\varepsilon_e) C_{ijkl}^0 \varepsilon_{kl})\,\mathrm{d}V, \\ &+ \int_V f_i^{\mathrm{B}} \delta u_i^{\mathrm{a}}\,\mathrm{d}V + \int_S f_i^{\mathrm{S}} \delta u_i^{\mathrm{a}}\,\mathrm{d}S - \frac{1}{2}\int_V \sigma_{ij}\left(\frac{\partial u_i^{\mathrm{a}}}{\partial x_j} + \frac{\partial u_j^{\mathrm{a}}}{\partial x_i}\right)\mathrm{d}V, \end{aligned} \tag{13}$$

where σ_{ij}^{a}, $\varepsilon_{ij}^{\mathrm{a}}$ and u_i^{a} are the various states of the adjoint structure to be determined; f_i^{B} and f_i^{S} denote the body forces and surface loadings, respectively. It is obvious that both the original functional, H and the new functional, H^*, are identical. By taking the derivative of Eq. (13) with respect to the design variable p, we have

$$\begin{aligned} \frac{\mathrm{d}H}{\mathrm{d}p} = &\int_V \frac{\partial h}{\partial p}\mathrm{d}V + \int_V \frac{\partial h}{\partial u_i}\frac{\partial u_i}{\partial p}\mathrm{d}V \\ &+ \int_V \sigma_{ij}^{\mathrm{a}}\left(\frac{\partial \varepsilon_{ij}}{\partial p} - \frac{1}{2}\left(\frac{\partial}{\partial x_j}\left(\frac{\partial u_i}{\partial p}\right) + \frac{\partial}{\partial x_i}\left(\frac{\partial u_j}{\partial p}\right)\right)\right)\mathrm{d}V \\ &+ \int_V \varepsilon_{ij}^{\mathrm{a}}\left(\frac{\partial \sigma_{ij}}{\partial p}\frac{\partial (K g(\varepsilon_{\mathrm{e}}) C_{ijkl}^0)}{\partial p}\varepsilon_{kl} - K g(\varepsilon_{\mathrm{e}}) C_{ijkl}^0 \frac{\partial \varepsilon_{\mathrm{e}}}{\partial p}\right)\mathrm{d}V \\ &- \frac{1}{2}\int_V \frac{\partial \sigma_{ij}}{\partial p}\left(\frac{\partial u_i^{\mathrm{a}}}{\partial x_j} + \frac{\partial u_j^{\mathrm{a}}}{\partial x_i}\right)\mathrm{d}V. \end{aligned} \tag{14}$$

In Eq. (14), the term, $(\partial(K g(\varepsilon_{\mathrm{e}}) C_{ijkl}^0)/\partial p)\varepsilon_{kl}$, can be further expanded by applying the chain rule and the derivative relation of Eq. (2) as

$$\begin{aligned} \frac{\partial (K g(\varepsilon_{\mathrm{e}}) C_{ijkl}^0)}{\partial p}\varepsilon_{kl} &= \frac{\partial K}{\partial p} g(\varepsilon_{\mathrm{e}}) C_{ijkl}^0 \varepsilon_{kl} + K C_{ijkl}^0 \varepsilon_{kl} \frac{\partial g(\varepsilon_{\mathrm{e}})}{\partial \varepsilon_{\mathrm{e}}}\frac{\partial \varepsilon_{\mathrm{e}}}{\partial \varepsilon_{pq}}\frac{\partial \varepsilon_{pq}}{\partial p} \\ &= \frac{\partial K}{\partial p} g(\varepsilon_{\mathrm{e}}) C_{ijkl}^0 \varepsilon_{kl} + K \frac{1}{\varepsilon_{\mathrm{e}}}\frac{\partial g(\varepsilon_{\mathrm{e}})}{\partial \varepsilon_{\mathrm{e}}} C_{ijkl}^0 \varepsilon_{kl} \varepsilon_{rs} C_{rspq}^0 \frac{\partial \varepsilon_{pq}}{\partial p}. \end{aligned} \tag{15}$$

Re-assigning indices of Eq. (15), substituting the result back into Eq. (14), we can collect the terms with $(\partial \sigma_{ij}/\partial p)$ and $(\partial \varepsilon_{ij}/\partial p)$ in the form of

$$\begin{aligned}\frac{\mathrm{d}H}{\mathrm{d}p} &= \int_V \frac{\partial h}{\partial p}\mathrm{d}V + \int_V \frac{\partial h}{\partial u_i}\frac{\partial u_i}{\partial p}\mathrm{d}V \\ &+ \int_V \frac{\partial \sigma_{ij}}{\partial p}\left(\varepsilon_{ij}^{\mathrm{a}} - \frac{1}{2}\left(\frac{\partial u_i^{\mathrm{a}}}{\partial x_j} + \frac{\partial u_j^{\mathrm{a}}}{\partial x_i}\right)\right)\mathrm{d}V \\ &+ \int_V \frac{\partial \varepsilon_{ij}}{\partial p}\left(\sigma_{ij}^{\mathrm{a}} - K\{g(\varepsilon_{\mathrm{e}})C_{ijkl}^{0} + \frac{1}{\varepsilon_{\mathrm{e}}}\frac{\partial g(\varepsilon_{\mathrm{e}})}{\partial \varepsilon_{\mathrm{e}}}C_{ijpq}^{0}\varepsilon_{pq}\varepsilon_{rs}C_{rskl}^{0}\}\varepsilon_{kl}^{\mathrm{a}}\right)\mathrm{d}V \\ &- \int_V \frac{1}{2}\sigma_{ij}^{\mathrm{a}}\left(\frac{\partial}{\partial x_j}\left(\frac{\partial u_i}{\partial p}\right) + \frac{\partial}{\partial x_i}\left(\frac{\partial u_j}{\partial p}\right)\right)\mathrm{d}V - \int_V \frac{\partial K}{\partial p}g(\varepsilon_{\mathrm{e}})\varepsilon_{ij}^{\mathrm{a}}C_{ijkl}^{0}\varepsilon_{kl}\,\mathrm{d}V.\end{aligned} \tag{16}$$

In Eq. (16), two integral terms leading with $(\partial\sigma_{ij}/\partial p)$ and $(\partial\varepsilon_{ij}/\partial p)$ can be eliminated by defining the adjoint structure as the followings:

$$\varepsilon_{ij}^{\mathrm{a}} = \frac{1}{2}\left(\frac{\partial u_i^{\mathrm{a}}}{\partial x_j} + \frac{\partial u_j^{\mathrm{a}}}{\partial x_i}\right), \tag{17}$$

$$\sigma_{ij}^{\mathrm{a}} = K\left\{g(\varepsilon_{\mathrm{e}})C_{ijkl}^{0} + \frac{1}{\varepsilon_{\mathrm{e}}}\frac{\partial g(\varepsilon_{\mathrm{e}})}{\partial \varepsilon_{\mathrm{e}}}C_{ijpq}^{0}\varepsilon_{pq}\varepsilon_{rs}C_{rskl}^{0}\right\}\varepsilon_{kl}^{\mathrm{a}}, \tag{18}$$

$$\int_V \frac{\partial h}{\partial u_i}\frac{\partial u_i}{\partial p}\mathrm{d}V = \int_V \frac{1}{2}\sigma_{ij}^{\mathrm{a}}\left(\frac{\partial}{\partial x_j}\left(\frac{\partial u_i}{\partial p}\right) + \frac{\partial}{\partial x_i}\left(\frac{\partial u_j}{\partial p}\right)\right)\mathrm{d}V. \tag{19}$$

One can find the first two terms of the right-hand side of Eq. (18) is the same as $C_{ijkl}^{\tan}$ in Eq. (10). By replacing them with $C_{ijkl}^{\tan}$ and assigning the sensitivity of $(\partial u_i/\partial p)$ as δu_i, Eqs. (18) and (19) can be re-written as,

$$\sigma_{ij}^{\mathrm{a}} = C_{ijkl}^{\tan}\varepsilon_{kl}^{\mathrm{a}}, \tag{20}$$

$$\int_V \frac{\partial h}{\partial u_i}\partial u_i\,\mathrm{d}V = \int C_{ijkl}^{\tan}\varepsilon_{kl}^{\mathrm{a}}\delta\varepsilon_{ij}\,\mathrm{d}V. \tag{21}$$

Combining Eqs. (17), (20) and (21), the adjoint system is formally defined. The stiffness matrix of the adjoint structure is found to be the tangent modulus matrix of the deformed structure under the original loading, and the adjoint loading is in the form of $\partial h/\partial u_i$. Finally, the sensitivity of the general displacement functional, H, can be expressed as the following form:

$$\frac{\mathrm{d}H}{\mathrm{d}p} = \int_V \frac{\partial h}{\partial p}\mathrm{d}V - \int_V \frac{\partial K}{\partial p}g(\varepsilon_{\mathrm{e}})\varepsilon_{ij}^{\mathrm{a}}C_{ijkl}^{0}\varepsilon_{kl}\,\mathrm{d}V, \tag{22}$$

where $\varepsilon_{ij}^{\mathrm{a}}$ is the only unkown and can be obtained from the strain field of adjoint structure. Once the sensitivity analysis is completed, the topology optimization is solved by a convex approximation method developed by Chickermane and Gea (1996) iteratively till the optimal layout is generated.

3.1. Optimization formulation

Compliant mechanism can be used in many different applications. Some applications are designed for repeated motion that small deformation and small strain would be desired. Others may elect the GA as the design objective, where large deformation of compliant structures should be considered. In this paper, we choose maximizing the MA as our objective function for compliant mechanism design. Therefore, compliant design with small deformation and linear/non-linear strain is used here.

To evaluate the MA of a mechanism, we attached a linear spring to the point s_0 in the direction n_i at which we plan to measure the output force. The choice of spring constant of the linear spring will affect the final design. Because the MA is our design objective, a stiff spring (large spring constant) is used here. The maximization of the MA becomes the maximization of the displacement of the linear spring given the applied load is a constant. This displacement field at the location s_0 can be written as,

$$u_{s_0} = \int_V \delta(s - s_0) u_i n_i \, \mathrm{d}V. \tag{23}$$

Comparing with the general displacement functional, Eq. (12), we found that the displacement kernel $k(u, p)$ is in the form of $\delta(s - s_0)\, u_i n_i$. Therefore, the applied load of the adjoint field, $\partial h/\partial u$, is a unit load at the point s_0 in the direction n_i, and the first term of the right-hand side of Eq. (22) is removed because of $\partial h/\partial p = 0$. The sensitivity of displacement field at the location s_0 is reduced to

$$\frac{\partial u_{s_0}}{\partial p} = -\int_V \varepsilon_{ij}^{\mathrm{a}} \frac{\partial K}{\partial p} g(\varepsilon_{\mathrm{e}}) C_{ijkl}^{0} \varepsilon_{kl} \, \mathrm{d}V. \tag{24}$$

Using the MA as the objective function, the optimization problem is formulated as

$$\text{maximize} \quad u_{s_0} = \int_V \delta(s - s_0) u_i n_i \, \mathrm{d}V$$

$$\text{subject to} \quad \int_V \rho \, \mathrm{d}V - \overline{W} \leq 0,$$

where ρ is the density of material and $\overline{W}$ is the maximum allowable weight of the structure. In Section 4, examples of compliant mechanism design considering material non-linearity will be presented using the maximal MA formulation.

4. Numerical examples

A force inverter design is studied in this section. A rectangular area 40 cm × 40 cm × 1 cm is considered as the design domain as shown in Figure 1. The top and bottom corners of the left side are fixed with pin joints and force is applied at the center of left edge. The small black region

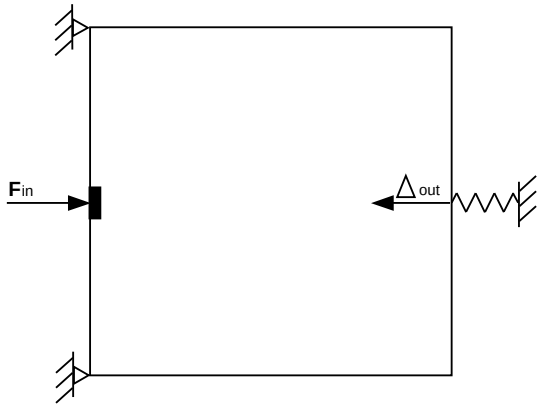

Figure 1. Design domain and boundary conditions for a force inverter design.

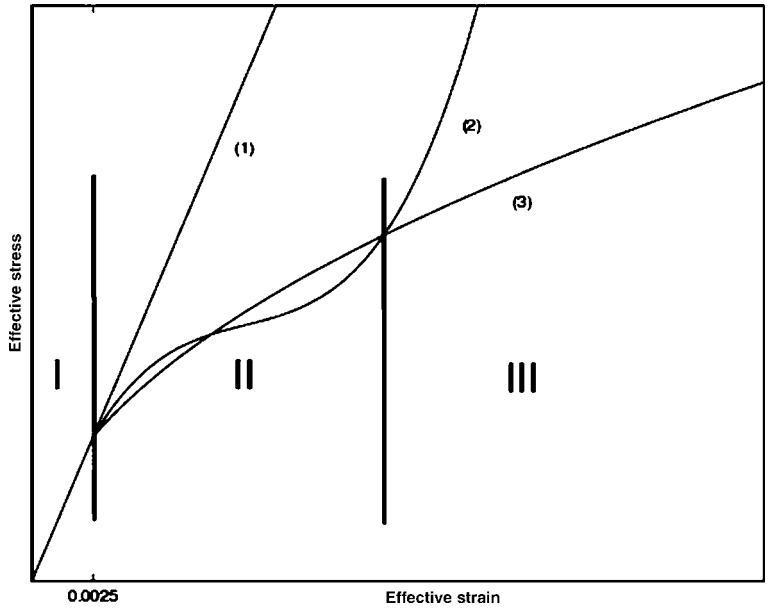

Figure 2. Stress–strain curves for (1) linear material, (2) elastomer like material model, and (3) power-law material.

where the input force applied at is considered as a nondesignable region. The output displacement (Δ_{out}) is measured at the center of right edge where a spring is attached to. As we stated previously, when MA is used as design objective the spring constant should be very stiff. In these examples, the spring stiffness is 1000 times of the structural material. Three material models are considered. Figure 2 shows the stress-strain relation of these material models: (1) represents linear stress-strain relation, $g(\varepsilon_e) = 1$; (2) denotes an elastomer like material where $g(\varepsilon_e) = 1 - 105\varepsilon_e + 4000\varepsilon_e^2$, and (3) is a power law material model in which $g(\varepsilon_e)$ is $\varepsilon_e^{0.5}$. Other

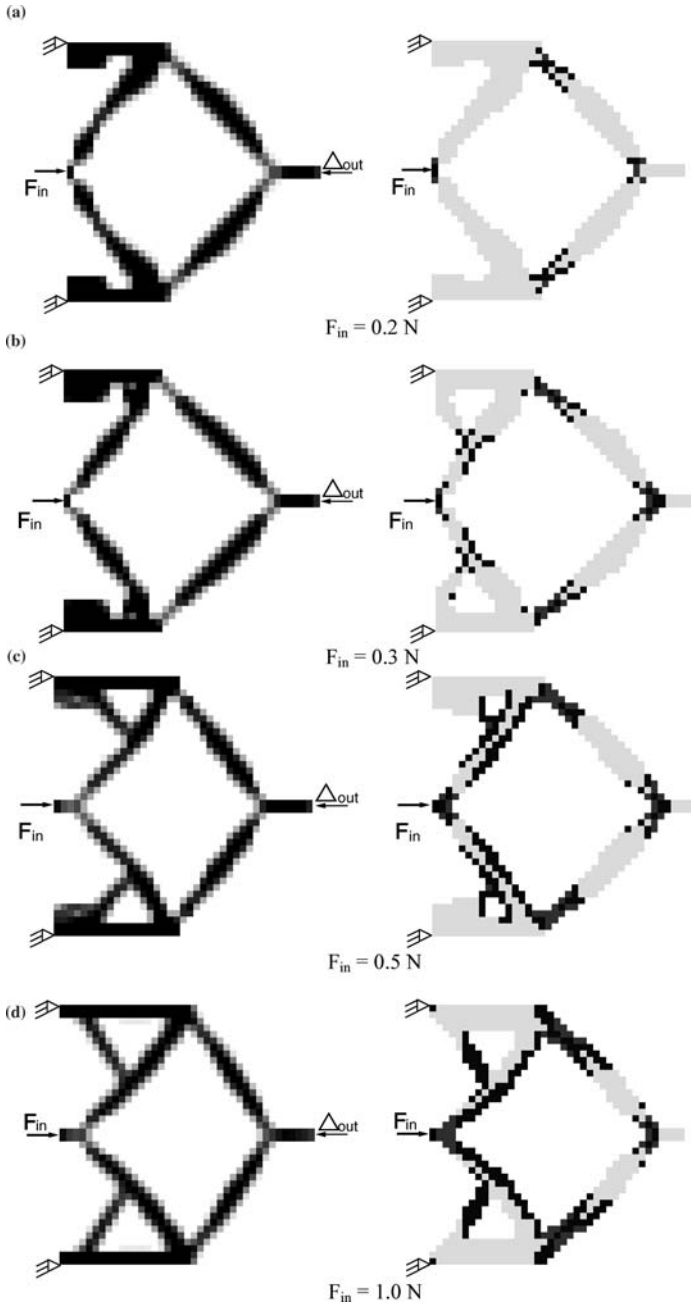

Figure 3. The optimal designs of a force inverter with elastomer like material under four different magnitudes of loads.

non-linear material models can also be implemented similarly. Linear stress–strain relation is assumed when the effective strain is less than 0.0025. The material properties of rectangular plate are: Young's modulus $E_0 = 300$ MPa, Poisson's ratio $v = 0.3$. This design is subjected to a 20% volume constraint.

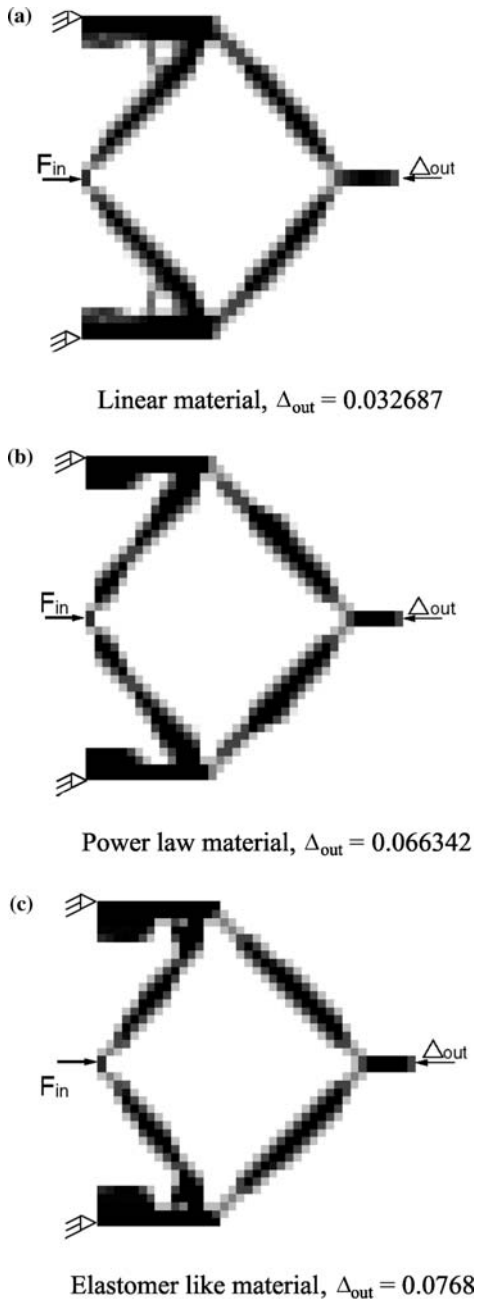

Figure 4. The optimal design of the force inverter for three different material models ($F_{in} = 0.3$ N).

4.1. Example 1: Force inverter with different extent of non-linearity

Since the elastomer like material model has the most nonlinear effects, we will study the optimal design with this material model in the first example under different applied forces. Four different magnitudes of loadings are applied in order to compare different material non-linearities.

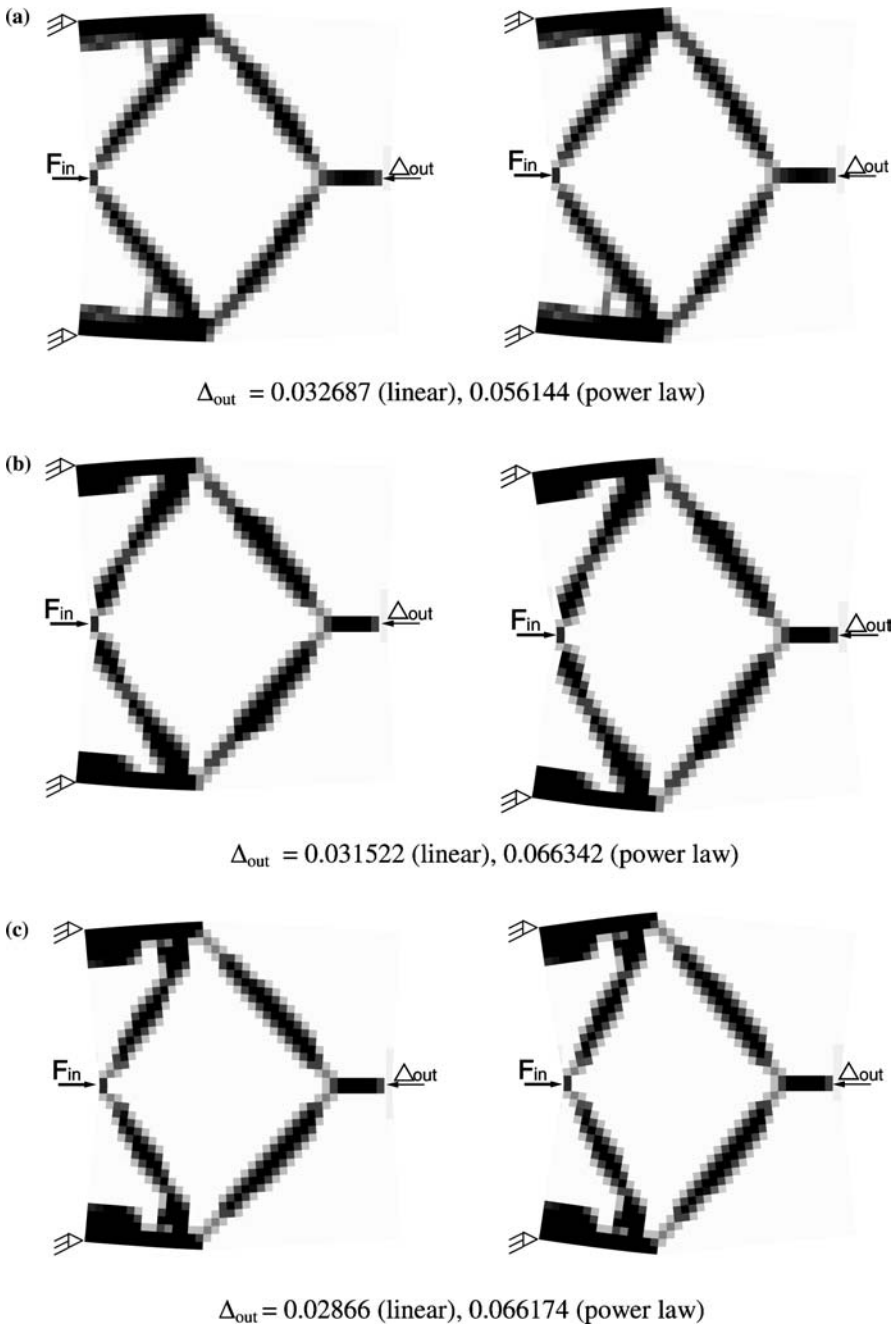

Figure 5. Deformed shapes and output displacements of optimal designs under linear analysis and power-law non-linear analysis.

These applied forces are 0.2, 0.3, 0.5, and 1 N. The optimal design (100th iteration) for each applied load are shown in the left column of Figure 3. As shown in the figure, the optimum designs are different with each applied load. The images at the right column of Figure 3 represent the magnitude of the effective strain. The grey scales correspond to strain level in the

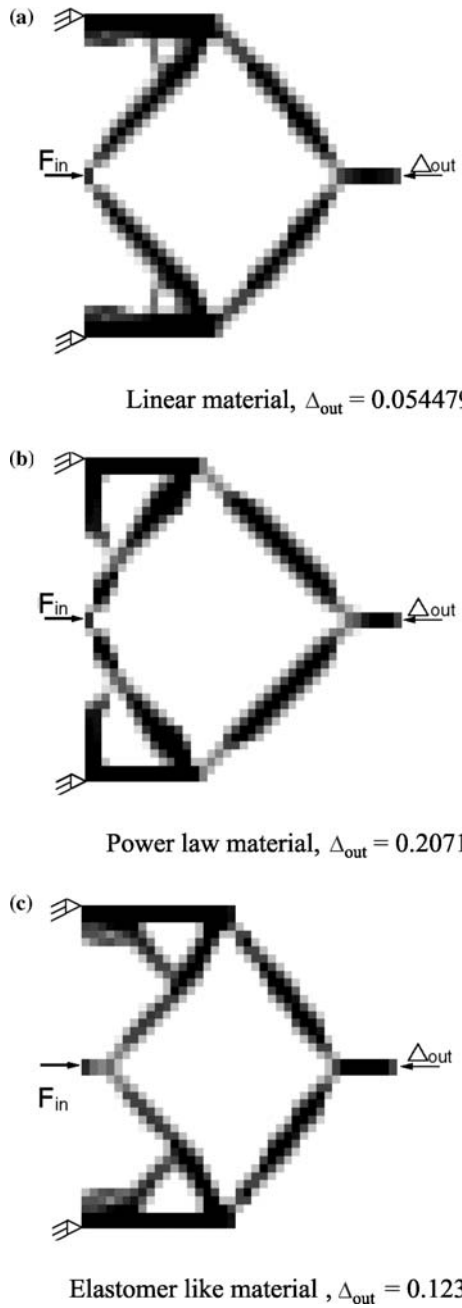

Figure 6. Optimal designs of the force inverter for three different material models ($F_{in} = 0.5$ N).

Figure 2. The darker regions represent the zone II and the zone III in Figure 2 and the light grey regions are for the linear region with the effective strain less than 0.0025. These images show that the non-linear regions start from the joint sections under 0.2 N and gradually expand to other parts under larger forces. They also showed that the optimal designs are changing from lumped compliant joints to distributed compliant structures as material non-linearity increased.

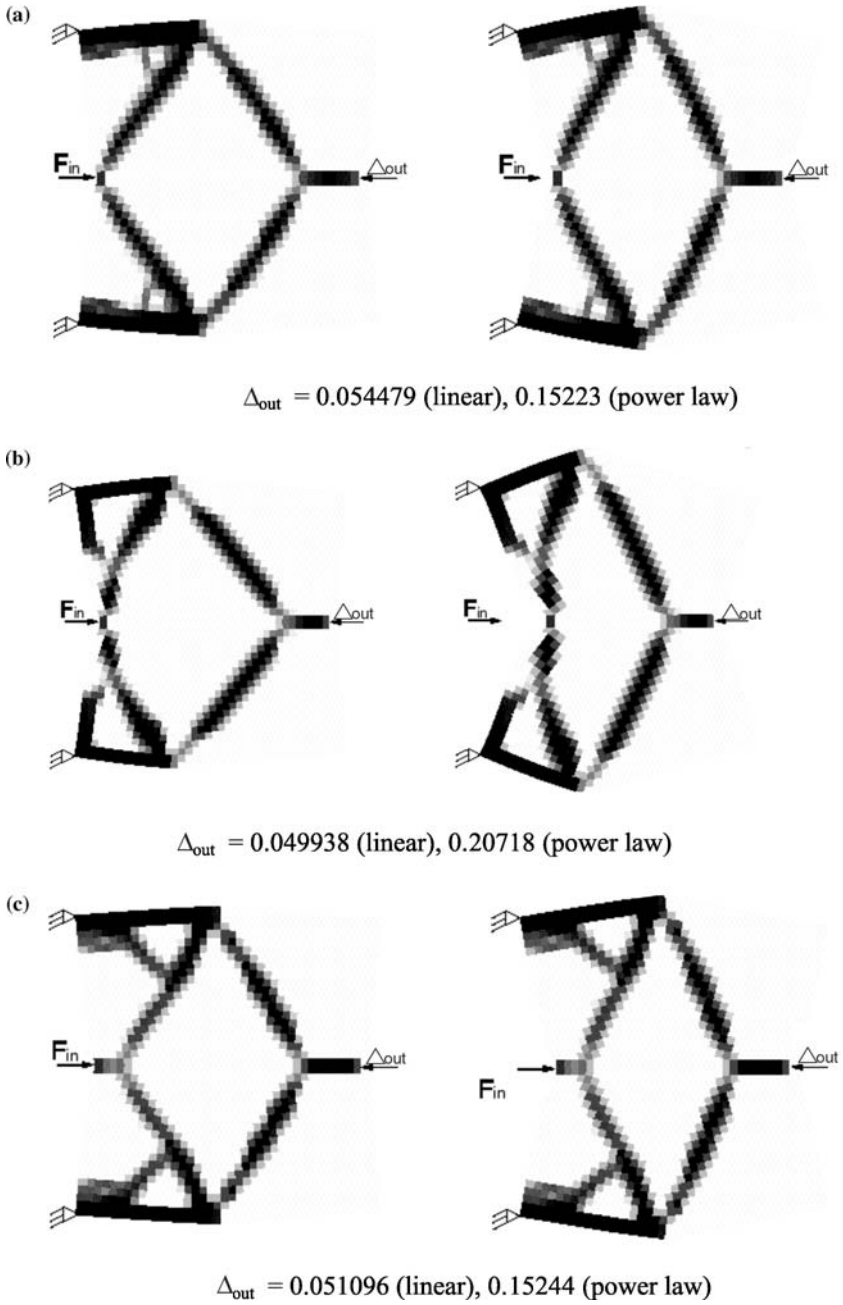

Figure 7. Deformed shapes and output displacements of optimal designs under linear analysis and power law nonlinear analysis.

4.2. Example 2: Force inverter under small loading

The second example is to design the force inverter. We will apply all three different material models discussed above. The applied force is 0.3 N. The optimized designs from each

material model are shown in Figure 4. Since the structural reactions are mainly in the linear range, the optimal designs are very similar even with different material model. To cross examine these solutions, we applied both linear material model (curve 1) and power-law material model (curve 3) to these designs and conducted finite element analyses. The deformed shapes and output displacements are shown in Figure 5. When the linear analysis is used, the optimal design from topology optimization with linear material model shows the best displacement as shown in the left column. However, if we replace the material model from linear material to power-law material, the second design outperforms the first one by 18%. These results confirm that material models in the topology optimization play a crucial role in determining the optimal configurations.

4.3. Example 3: Force inverter under large loading

In the third example, the applied force is increased to 0.5 N in order to examine the non-linear behaviors of materials. Figure 6 shows the optimal designs for three material models. The optimal design of the linear material is exactly same as that of the second example. But, the optimal designs of the power-law material and elastomer like material show additional structural members to prevent the weak members from large deformations. We also applied linear material model and power-law material model to these optimal solutions to verify their optimalities as we did in the second example and the results are shown in Figure 7. The same conclusion is found here: material models will change the optimal configurations.

5. Conclusion

In this paper, the sensitivity analysis of a general displacement functional for non-linear material models using the adjoint method has been derived. Since we are focusing on the MA of compliant mechanisms, different nonlinear material models are studied here. Three different material models are used to compare the optimal topology. From the numerical examples, we found that the compliant designs are changing from "lumped compliance" to "distributed compliance" as the structures experience more non-linear behaviors. This finding will provide engineers insight on designing compliant mechanism with MA applications. We also showed that different material models will produce different optimal designs. This functionality will also give engineers flexibility on selecting materials for compliant mechanisms. To further extend this work, study on combining material and geometrical nonlinearities has been initiated.

References

Ananthasuresh, G.K., Kota, S. and Kikuchi, N. (1994). Strategies for systematic synthesis of compliant MEMS. *DSC-Vol. 55–2, 1994 ASME Winter Annual Meeting,* pp. 677–686.

Ananthasuresh, G.K. and Kota, S. (1996). The Role of Compliance in the Design of MEMS. *Proceedings of the 1996 ASME Design Engineering Technical Conferences, 96-DETC/MECH-1309*.

Bathe, K.J. (1996), *Finite Element Procedures,* Prentice-Hall, New Jersey.

Belytschko, T., Liu, W.K. and Moran, B. (2000). *Nonlinear Finite Elements for Continua and Structures,* John Wiley & Sons.

Bendsøe, M.P., Guedes, J.M., Plaxton, S. and Taylor, J.E. (1996). Optimization of structure and material properties for solids composed of softening material. *International Journal of Solids and Structures* **33**(12), 1799–1813.

Bruns, T.E., Sigmund, O. and Tortorelli, D.A. (2002). Numerical methods for topology optimization of nonlinear elastic structures that exhibit snap-through. *International Journal for Numerical Methods in Engineering* **55**(10), 1215–1237.

Bruns, T.E. and Tortorelli, D.A. (2001). Topology optimization of non-linear elastic structures and compliant mechanisms. *Computer Methods in Applied Mechanics and Engineering* **190**, 3443–3459.

Buhl, T., Pedersen, C.B.W. and Sigmund, O. (2000). Stiffness design of geometrically nonlinear structures using topology optimization. *Structural Multidisciplinary Optimization* **19**, 93–104.

Chen, W.F. (1994). *Constitutive Equations for Engineering Materials, Vol. 2: Plasticity and Modeling,* Elsevier.

Chickermane, H. and Gea, H.C. (1996). Structural optimization using a new local approximation method. *International Journal for Numerical Methods in Engineering* **39**(5), 829–846.

Frecker, M.I., Ananthasuresh, G.K., Nishiwaki, S., Kikuchi, N., and Kota, S. (1997). Topological synthesis of compliant mechanism using multi-criteria optimization. *ASME Journal of Mechanical Design* **119**, 238–245.

Howell, L.L. and Midha, A. (1993). Compliant Mechanisms, Section 9.10, *Modern Kinematics: Developments in the Last Forty Years* (editor: A. Erdman), Wiley, New York, pp. 422–428.

Jog, C. (1996). Distributed-parameter optimization and topology design for non-linear thermoelasticity. *Computer Methods in Applied Mechanics and Engineering* **132**, 117–134.

Larsen, U.D., Sigmund, O. and Bouwstra, S. (1997). Design and fabrication of compliant mechanisms and material structures with negative poisson's ratio. *Journal of Microelectromechanical Systems* **6**(2), 99–106.

Maute, K., Schwarz, S. and Ramm, E. (1998). Adaptive topology optimization of elastoplastic structures. *Structural Optimization* **15**,81–91.

Nishiwaki, S., Frecker, M.I., Min, S. and Kikuchi, N. (1998). Topology optimization of compliant mechanisms using the homogenization method, *International Journal for Numerical Methods in Engineering* **42**(3), 535–559.

Pedersen, P. (1998), Some general optimal design results using anisotropic, power law nonlinear elasticity. *Structural Optimization,* **15**, 73–80.

Pedersen, C.B.W. Buhl, T. and Sigmund, O. (2001), Topology synthesis of large-displacement compliant mechanisms. *International Journal for Numerical Methods in Engineering*, 50, 2683–2705.

Saxena, A. and Ananthasuresh, G.K. (2000). On an optimal property of compliant topologies. *Structural and Multidisciplinary Optimization* **19**, (1), 36–49.

Sigmund, O. (1997). On the design of compliant mechanisms using topology optimization. *Mechanics of Structures and Machines* **25**(4), 493–524.

Sigmund, O. (2001a), Design of multiphysics actuators using topology optimization—Part I: One-material structures. *Computer Methods in Applied Mechanics and Engineering* **190**, 6577–6604.

Sigmund, O. (2001b). Design of multiphysics actuators using topology optimization—Part II: Two-material structures. *Computer Methods in Applied Mechanics and Engineering* **190**, 6605–6627.

Song, J.O. (1986). An optimization method for crashworthiness design. *Proceedings of the Sixth International Conference on Vehicle Structural Mechanics, Detroit, MI,* 39–46.

Swan, C.C. and Arora, J.S. (1997). Topology design of material layout in structured composites of high stiffness and strength. *Structural Optimization* **13**, 45–59.

Swan, C.C. and Kosaka, I. (1997). Voigt-Reuss topology optimization for structures with nonlinear material behaviors. *International Journal for Numerical Methods in Engineering* **40**, 3785–3814.

Vander Lugt, D.A., Fischer, R.A. and Chen, R. (1987). Passenger car frontal barrier simulation using nonlinear finite element methods. *SAE Technical Paper 871958, Passenger Car Meeting, Dearborn, MI.*

Yin, L. and Ananthasuresh, G.K. (2002). A novel formulation for the design of distributed compliant mechanisms, *Mechanics Based Design of Structures and Machines* **31** (2), 151–179.

Yuge, K. and Kikuchi, N. (1995), Optimization of a frame structure subjected to a plastic deformation, *Structural Optimization* **10**, 197–208.